NASA Technical Memorandum 88786

Analysis of the Gas Particle Radiator

Donald L. Chubb
Lewis Research Center
Cleveland, Ohio

July 1986

NASA

ANALYSIS OF THE GAS PARTICLE RADIATOR

Donald L. Chubb
National Aeronautics and Space Administration
Lewis Research Center
Cleveland, Ohio 44135

SUMMARY

Theoretical performance of a new space radiator concept, the gas particle radiator (GPR), is calculated. The GPR uses a gas containing emitting, submicron particles as the radiating media. A transparent window contains the gas particle mixture around the solid radiator emitting surface. A major advantage of the GPR is that large emissivity ($\varepsilon_T \geq 0.8$) is achieved without the use of emissive coatings. A radiation heat transfer analysis shows that for a modest volume fraction ($\sim 10^{-4}$) of submicron particles and gas thickness ($\sim$1 cm) the emissivity, ε_T, is limited by the window transmittance. Besides determining the emissivity, the window is the critical element for making it possible for the GPR to have lower mass than a tube type radiator. The window acts as a "bumper" to provide meteoroid protection for the radiator wall. The GPR was compared to a proposed titanium wall, potassium heat pipe radiator. For both radiators operating at a power level of 1.01 MW at 775 K it was calculated that the GPR mass was 31 percent lower than the heat pipe radiator.

E-2639-1

I. INTRODUCTION

High specific power (power radiated/radiator mass), small area and long lifetime are the desirable characteristics of a space radiator. These characteristics will be attained if a low mass and high emissivity, ε_T, that is stable for long periods (7 to 10 yr) can be achieved.

For a tube type radiator (either a heat pipe or a pumped loop) high emissivity ($\varepsilon > 0.8$) is achieved by the use of emissive coatings. Adhesion and emissive stability of these coatings must be obtained for long periods of time if a tube type radiator is to be a successful space radiator. Generally, the largest mass portion of a tube radiator is the armor that must be used to protect against meteoroid penetration.

The gas particle radiator (GPR) is a new concept that has the potential for long lifetime, high emissivity with lower mass than tube radiators. Figure 1 is a conceptual drawing of the GPR. A gas which contains a suspension of fine particles is contained in a sealed volume between the tube radiator

and an outer window that are separated by a distance, D. On start-up of the radiator a temperature gradient will exist across the gas. This temperature gradient will induce a gas flow that will distribute the particles throughout the gas. However, this will have to be demonstrated for a successful GPR. In the micro-gravity of space the particles should remain in suspension. Uniform particle distribution is critical to obtaining high emissivity. Therefore, it will be necessary to prove uniform distribution can be established before a GPR is a viable space radiator. If the window is transparent to the emitted radiation the gas particle mixture will yield a high, stable emissivity. Past investigations (ref. 1) of a soot-containing flame, that is similar to the gas particle mixture of the GPR, have yielded large emittances. Obtaining high emissivity without the use of emissive coatings is a major advantage of the GPR.

It would appear that the addition of the gas-particle mixture plus a surrounding window will result in a larger mass for the GPR than a tube radiator. However, the addition of the window "bumper" will provide meteoroid protection for the emitting tube. This window "bumper" means the combined thickness (window + tube) may be significantly less than the tube-only thickness and still provide the same meteoroid protection (refs. 2 and 3). Therefore, the GPR may have a lower mass than a tube radiator.

The major problem for the GPR is finding a suitable window material. As will be shown, it is the window transmittance that limits the emissivity. There are suitable choices for the gas and particle materials. However, there is a need to experimentally verify the emissivities predicted in this study.

Suitable window materials and a verified emissivity are the critical issues for the GPR. However, even if these issues can be resolved satisfactorily there are other design problems that will also have to be solved. It will be necessary to provide a seal between the window and the radiating surface. Also, provision will have to be made for the difference in thermal expansion of the window material and the metallic radiating surface material. The analysis and results for the emissivity of the GPR are presented in the following section. A discussion of possible window materials is presented in section III, and a mass comparison is made between the GPR and tube type radiators in section IV. Finally, conclusions are presented in section V.

II. EMISSIVITY OF GAS PARTICLE RADIATOR

A number of studies (summarized in ref. 1) of the emittance of soot-containing gases have been carried out. These investigations yield large

emittances for modest amounts of soot concentration. Seeding with small particles has also been proposed to increase gas absorption of incident radiation (ref. 4) or as a means of shielding a surface from incident radiation (refs. 5 and 6). The success of the GPR depends on large emittance (or absorption) of the gas-particle mixture, similar to these concepts. In reference 4 large absorption was measured as a function of wavelength, λ, in the range $0.2 \leq \lambda \leq 1$ μm for carbon, aluminum oxide, hafnium carbide, and tungsten particles suspended in water. Particle diameters ranged from 0.02 to 2 μm.

The total emissivity, ε_T, for the GPR is derived in Appendix A. The most important approximations used in this derivation are that the gas, particles, and radiator surface are at the same temperature and the absorption coefficient, k_λ^g, of the gas-particle medium is uniform and is determined by the particle optical properties. It is assumed that the gas is transparent to the emitted radiation. Also, the emissivity of the radiator surface, ε_p, is neglected. Two ranges of particle size are considered in Appendix A. For particles of small radius, r_d, ($r_d/\lambda < 1$) the following absorption coefficient is assumed,

$$k_\lambda^g = \frac{K}{\lambda}\varphi, \qquad \frac{r_d}{\lambda} < 1 \tag{1}$$

where K is a constant, λ is wavelength and φ is the volume fraction of particles in the gas-particle medium. Equation (1) is an absorption coefficient that fits the emittance results for soot-containing gases (refs. 1 and 6). For large particles ($r_d/\lambda > 1$) the absorption cross section, σ_λ^a, for the particles is assumed to be equal to the particle cross-sectional area, πr_d^2. Therefore, the absorption coefficient in this case is the following.

$$k_\lambda^g = n_d \sigma_\lambda^a = \frac{3}{4}\frac{\varphi}{r_d}, \qquad r_d/\lambda > 1 \tag{2}$$

Where n_d is the particle number density.

$$n_d = \frac{\varphi}{V_d} = \frac{\varphi}{\frac{4}{3}\pi r_d^3} \tag{3}$$

For the emission temperature range of interest for the GPR (300 to 1200 K), more than 90 percent of the radiation will be in the range $1 \leq \lambda \leq 75$ μm. Therefore, the small particles must satisfy $r_d < 1$ μm and the large particles are defined by $r_d > 75$ μm.

As mentioned above, it was assumed that the gas and particles are at the same temperature. The validity of this approximation is examined in Appendix B. For small particles ($r_d < \ell_g$ where ℓ_g is the mean free path) the heat transfer between the gas and particles will be determined by free-molecular flow, whereas for large particles ($r_d \geq \ell_g$) the heat transfer is determined by continuum flow. Results for the temperature difference, $\Delta T = T_g - T_{rad}$, where T_{rad} is the particle temperature at a gas pressure, $p_g = 0.1$ atm, and a particle temperature, $T_{rad} = 1000$ K are calculated in Appendix B. For both small particles (free molecular flow) and large particles (continuum flow) $\Delta T < 0.01\ T_{rad}$. Under these conditions of pressure and temperature it appears reasonable to neglect the difference in temperature between the gas and the particles.

An important part of the ε_T calculation is the window specular transmission, τ_λ^W. For most window materials τ_λ^W can be approximated by a square wave (ref. 7). Therefore, equation (A31) was used to approximate τ_λ^W. Using this window approximation and the assumptions described above the following results for ε_T were derived in Appendix A for large particles,

$$\varepsilon_T = \tau_W\left(1 - e^{-\beta}\right) F_{o-\lambda_u T_p}, \qquad r_d \geq 75\ \mu m \tag{4}$$

and for small particles,

$$\varepsilon_T = \tau_W \left\{ F_{o-\lambda_u T_p} - \frac{90}{\pi^4}\left(\frac{1}{\gamma + 1}\right)^4 Q\left[\frac{2hc}{k\lambda_u T_p}(\gamma + 1)\middle| 8\right]\right\} \tag{5}$$

where

$$\beta = 2.7\,\frac{\varphi D}{r_d}, \qquad r_d \geq 75\ \mu m \tag{6}$$

$$\gamma = \frac{3.6KkT_p}{hc}\,\varphi D, \qquad r_d \leq 1\ \mu m \tag{7}$$

The quantities $F_{o-\lambda_u T_p}$ and $Q[x^2|\upsilon]$ are integral functions given by equations (A36) and (A40). Other quantities appearing in equations (4) to (7) are the speed of light, c, Plank's constant, h, and Boltzmann's constant, k, (hc/k = 14,388 μm-K). The window transmission, τ_W, is the magnitude of τ_λ^W between the lower, λ_ℓ, and upper, λ_u, cutoff wavelengths on the window transmission, (eq. (A31)), and T_p is the temperature of the emitting radiation surface.

In figure 2, ε_T/τ_w for large particles (eq. (4)) is shown as a function of $\lambda_u T_p$ for several values of β. For large values of β (>4) the exponential term in equation (4) is negligible and $\varepsilon_T \rightarrow \tau_w F_{o-\lambda_u T_p}$. In this case ε_T is determined entirely by the window transmission. For small particles (eq. (5)) the quantity ε_T/τ_w is shown as a function of $\lambda_u T_p$ for several values of γ. Similar to the case for large particles, when γ is large ($\gamma > 1$) $\varepsilon_T \rightarrow \tau_w F_{o-\lambda_u T_p}$. Therefore, for both small and large particles the total emissivity will be determined by the window transmission if the parameters β and γ are large.

Consider the volume fraction, φ, necessary to attain large β (>4) and large γ (>1). In the case of large particles (eq. (6)) the smallest r_d yields the largest value of β. Therefore, assume $r_d \approx 75$ μm and for a practical GPR, $D \approx 1$ cm. As a result $\varphi > 0.01$ is required to attain $\beta > 4$. Now consider small articles (eq. (7)). The parameter, K, is in the range 4 to 6 μm/μm for soot (ref. 1). Therefore, assume $K \approx 5$ μm/μm. Also, considering the lowest temperature of interest $T_p \approx 300$ K and again using $D \approx 1$ cm the volume fraction necessary to attain $\gamma > 1$ is $\varphi > 2.7\text{x}10^{-4}$. A much smaller volume fraction ($\varphi > 10^{-4}$) is required to attain $\gamma > 1$ for small particles than to attain $\beta > 4$ for large particles ($\varphi > 0.01$). The smallest φ is most desirable for the GPR since the total particle mass will be a minimum. Therefore, the use of small particles ($r_d < 1$ μm) will yield the same ε_T with less mass than with large particles ($r_d > 75$ μm).

Based on the above discussion, $\varphi > 10^{-4}$, should insure that the maximum feasible emissivity $\left(\varepsilon_T \rightarrow \tau_w F_{o-\lambda_u T_p}\right)$ will be attained for small particles. However, as figures 2 and 3 show, only for $\lambda_u T_p \geq 7\text{x}10^3$ μm K will ε_T/τ_w be large ($\varepsilon_T/\tau_w > 0.8$). At $T_p \approx 300$ K this means $\lambda_u \geq 20$ μm. There are few materials with good transmission at wavelengths this long. Therefore, the GPR will be more appropriate for higher temperatures. Window materials that can possibly be used for the GPR will be discussed in the next section.

III. WINDOW MATERIALS

As shown in the previous section it is the window transmission that determines the GPR emissivity. Therefore, it is critical to have a window with large transmittance in the wavelength range of interest. Since the radiator temperatures of interest are 300 to 1200 K the majority of emitted radiation will be in the infrared ($\lambda > 1$ μm). Therefore, window materials such as ordinary glass will not be suitable.

Several materials are listed in Table I that have excellent transmittance in the infrared. The optical transmittances of all materials except the heavy metal fluoride glasses, (HMFG), were obtained from reference 7. All the other properties except the yield stress were obtained from reference 8. The yield stresses were obtained from the noted references. All properties of the HMFG systems were obtained from reference 9. Most of the materials shown in Table I are alkali halides, which are soluble in water. Although water solubility would be a serious problem for operation in a water-containing atmosphere, operation in the vacuum of space should relieve this problem. Manufacturing large pieces of the alkali halides of the required optical properties may be a problem. However, continuous single crystal fibers of cesium bromide and other alkali halides with excellent transmittance have been manufactured (ref. 10).

The window material in the GPR must be strong enough to contain the gas particle mixture. Since very thin windows (<1 mm) are desirable the yield stress of the material will determine the limiting thickness. Yield stresses of the pure alkali halides is low. However the addition of halide impurities (refs. 11 and 12) results in significant increases in the yield stress. Whether the optical properties are altered by these impurities is not stated in references 11 and 12.

If the GPR is to become a workable concept an appropriate window material must be developed. Alkali halides are possible candidates. However, manufacturing thin sheets of these materials with sufficient yield strength must be demonstrated.

IV. MASS COMPARISON BETWEEN GAS PARTICLE RADIATOR AND TUBE RADIATOR

In an earlier section the conditions necessary to obtain large emissivity for the GPR were described. Besides large emissivity, low mass is the other important characteristic of a space radiator. In this section a mass comparison is presented between the GPR and tube type radiators.

The total mass, M_T of the GPR can be written as follows,

$$M_T = \alpha_T A_T + M_a \tag{8}$$

where α_T (kg/m^2) is the specific mass of the radiating surface, A_T (m^2) is the total radiating surface area and M_a is the mass of auxiliary components such as

the radiator working fluid and manifolding. Similarly, the total mass of a tube type radiator can be written as follows.

$$M_o = \alpha_o M_o + M_{a_o} \tag{9}$$

Dividing equation (8) by (9) the ratio of total masses is obtained.

$$\frac{M_T}{M_o} = \frac{\alpha_T A_T}{\alpha_o A_o}\left(\frac{1 + \frac{\alpha_T'}{\alpha_T}}{1 + \frac{\alpha_o'}{\alpha_o}}\right) \tag{10}$$

The auxiliary masses (M_a and M_{a_o}) are assumed proportional to the radiating areas.

$$M_a = \alpha_T' A_T \tag{11a}$$

$$M_{a_o} = \alpha_o' A_T \tag{11b}$$

Assume the GPR is formed by adding a gas particle mixture surrounded by a window to the tube type radiator. In that case a relation for the ratio of specific masses, α_T/α_o, is derived in Appendix C. The result is given by equation (C14). The area ratio, A_T/A_o, is determined by the power radiated. For a space radiator redundant area must be included to make up for radiator area that is lost as a result of meteoroid penetration. As mentioned in the Introduction, the window for the GPR acts as a bumper to protect the radiator surface. Therefore, if the window is penetrated by a meteoroid the radiating gas particle mixture is lost but the radiator surface will remain operable. This remaining radiator surface will have an emissivity, ε_T', that is less than the the GPR emissivity, ε_T. For the tube type radiator all area that is affected by a meteoroid penetration is lost as a radiating surface. The radiator area, A_s, with emissivity, ε_o, that remains operative at the end of the mission must be sufficient to emit the entire radiator load. In the case of the GPR the radiator load at the end of the mission is shared by two areas. They are the area, A_s with emissivity ε_T that does not suffer meteoroid penetration and the area, $A_T - A_S$, with emissivity ε_T' that has lost the gas particle mixture as a result of meteoroid penetration. If both the GPR and the tube type

radiator are operating with the same load and with the same view factor the following relation is obtained for the area ratio, A_T/A_o.

$$\frac{A_T}{A_o} = \frac{\varepsilon_o}{\varepsilon_T}\left[\frac{1}{1 + \frac{\varepsilon_T'}{\varepsilon_T}\left(\frac{1}{r} - 1\right)}\right] \tag{12}$$

In obtaining equation (12) the same redundancy factor, r, was assumed for the GPR and the tube type radiator.

$$r = \frac{A_s}{A_T} = \frac{A_{s_o}}{A_o} \tag{13}$$

Using equations (C14) and (12) the following result is obtained.

$$\frac{\alpha_T A_T}{\alpha_o A_o} = \left(\frac{\varepsilon_o}{\varepsilon_T}\right)\left(\frac{t_p}{t_o}\right)\left[\frac{1}{1 + \frac{\varepsilon_T'}{\varepsilon_T}\left(\frac{1}{r} - 1\right)}\right]\left[\mu_w\left(\frac{t_w}{t_p}\right) + \mu_g\left(\frac{D}{t_p}\right) + \mu_s\left(\frac{t_s}{t_p}\right) + 1\right] \tag{14}$$

where t_p is the thickness of the radiator tube of the GPR, t_o is the thickness of the radiator tube of the tube type radiator, t_w is the thickness of the window, t_s is the thickness of the window attachment member, and μ_w, μ_g, and μ_s are defined in Appendix C.

The $\mu_g\ (D/t_p)$ term is the mass of the gas particle mixture, the $\mu_w\ (t_w/t_p)$ term is the mass of the window, and the $\mu_s\ (t_s/t_p)$ term is the mass of the attachment member. The μ_g term can be neglected in equation (14) for small volume fractions ($\varphi \leq 10^{-4}$). Referring to equation (C17), $\mu_g\ (D/t_p) \sim \varphi\ (D/t_p)$, since $\rho_g << \rho_o$ and $\rho_d \approx \rho_o$. Therefore, if $\varphi \approx 10^{-4}$ and $D/t_p \approx 10^2$, $\mu_g\ (D/t_p) \approx 10^{-2}$.

As mentioned in the Introduction, the window of the GPR will act as a bumper against meteoroid penetration of the radiating surface. Therefore, the total thickness, $t_p + t_w$, can be significantly less than t_o and still provide the same meteoroid protection. For high speed meteoroids (~20 km/sec) the bumper fragments and vaporizes the meteoroid dispersing the fragments over a large area so that penetration of the main wall does not occur. Data from Explorer 46 (ref. 3) using a stainless steel bumper and main wall indicated that $t_p + t_w \approx t_o/6.9$ provided the same meteoroid protection as t_o. In this case t_w is the bumper thickness. Since meteoroid penetration depth is not sensitive to the target material (refs. 13 and 14) it is expected that similar

behavior will exist for other materials. In reference 3 the optimum distribution of mass between the bumper and the main wall was calculated to be $t_w/t_p = 0.1$ to 0.2. Using this result together with $t_p + t_w = t_o/6.9$ the following is obtained.

$$0.12 \leq \frac{t_p}{t_o} \leq 0.13 \tag{15}$$

Therefore, unless $\varepsilon_o/\varepsilon_T \gg 1$, the magnitude of $\alpha_T A_T/\alpha_o A_o$ (eq. (14)) will be small if t_p/t_o is given by equation (15). If $\alpha_T A_T/\alpha_o A_o$ is small then a significant reduction in the mass ratio M_T/M_o, (eq. (10)) will result.

Now consider a comparison between a proposed heat pipe radiator (ref. 14) and a hypothetical GPR. A cross section of this radiator and this radiator with a gas-particle mixture and window added is shown in figure 4. The heat pipe radiator of reference 14 uses a flat plate radiating surface of titanium at $T_p = 775$ K with an emissivity, $\varepsilon_o = 0.9$ and a total radiated power of 1.01 MW. The radiator wall thickness ($t_o = 0.60$ mm) and redundancy, ($r = 321/360$) was designed to provide a lifetime of 7 yr with 0.99 probability of survival against meteoroid penetration.

The emitting gas particle mixture for the hypothetical GPR consists of small carbon particles ($\rho_d = 1.6$ gm/cm^3) and helium. Helium will be transparent to the emitted particle radiation. Also, its low molecular weight and thus high heat transfer coefficient (eq. (B19)) means there will be a negligible temperature difference between the helium and carbon particles. Since it is desirable to make the window as thin as possible the helium gas pressure should be as low as possible. The helium pressure was set to obtain $\Delta T < 0.01\ T_{rad}$, where $\Delta T = T_g - T_{rad}$ is the temperature difference between the helium gas (T_g) and the particles (T_{rad}). Using equations (B19), (B27a), and (B28) for $T_g = 775$ K and $\varepsilon_s/\alpha \approx 1$, the helium pressure requirement is, $p_g \geq 2000$ n/m^2 (15 torr).

Window material was chosen to obtain high emissivity. From figure 3 for $\gamma > 1$ it can be seen that $\lambda_u T_p \geq 10^4$ μm K for $\varepsilon_T/\tau_w \geq 0.9$. Therefore, for $T_p = 775$ K, $\lambda_u \geq 13$ μm. Referring to Table I we see there are several materials that satisfy $\lambda_u \geq 13$ μm and also have a melting point significantly above 775 K. For the hypothetical GPR sodium chloride was chosen as the window material. Whether NaCl can be produced in large area, thin sheets suitable for a GPR is a question that is yet to be answered.

Consider the emissivity that is possible with the carbon particle, helium mixture, and NaCl window. The parameters, γ (eq. (7)), and $\lambda_u T_p$ determine

the emissivity, ε_T/τ_w. For D = 1 cm, K = 5 μm/μm and T_p = 775 K, then $\gamma \geq 1$ for $\varphi > 1.03\text{x}10^{-4}$. Therefore, as long as $\varphi > 1.03\text{x}10^{-4}$ the $\gamma > 1$ curve in figure 3 can be used to obtain ε_T/τ_w. For NaCl λ_u = 15 μm and $\tau_w > 0.9$ (Table I). Using figure 3 for $\lambda_u T_p = 1.16\text{x}10^4$ μm K, $\gamma > 1$, and $\tau_w = 0.9$ results in $\varepsilon_T = 0.84$. Thus ε_T is slightly less than the assumed emissivity, $\varepsilon_o = 0.90$, of the heat pipe radiator. When the area ratio, A_T/A_o (eq. (12)), is calculated using $\varepsilon_T' = 0.3$ and r = 321/360 however, it is found that $A_T/A_o = 1.03$. The increase in area resulting from $\varepsilon_o/\varepsilon_T > 1$ is nearly compensated for by the redundant area savings, $[1 + \varepsilon_T'/\varepsilon_T \ (1/r - 1)]^{-1}$ term in equation (12).

As already mentioned the thickness of the heat pipe wall is t_o = 0.6 mm. Applying equation (15) results in $0.072 < t_p < 0.078$ mm. Although it may be possible to use such a thin wall thickness, t_p = 0.1 mm was arbitrarily chosen as a practical limit on t_p. This same limit was also chosen for t_w, so that $t_w = t_p = 1/6\ t_o$ = 0.1 mm. With $t_w + t_p$ = 0.2 mm meteoroid protection will be more than required, ($t_w + t_p \approx t_o/6.9$). Titanium of thickness, $t_s = t_p$ = 0.1 mm, will also be assumed for the connecting member between the plate and window.

As well as providing meteoroid protection, the window and emitting plate must be of sufficient thickness to contain the pressure loads of the helium gas and heat pipe fluid. The window must contain the helium pressure of 15 torr. If the distance, L ≈ 20 cm (eq. (C1)), then the maximum shear stress (p_g L/t_w) will be 4 n/mm^2 (600 psi). This is well within the yield stress for NaCl with impurities added to increase the yield strength (Table I). The potassium heat pipe of reference 14 operates at a pressure of 4124 n/m^2 (31 torr). Therefore, the pressure load on the titanium is p_H = 31 - 15 = 16 torr, which for heat pipe length (ref. 14), L' = 5.15 m, produces a maximum shear stress ($p_H L'/t_p$) of $1.1\text{x}10^2$ n/mm^2 ($1.6\text{x}10^4$ psi) well within the yield stress ($1.55\text{x}10^5$ psi).

Using the materials, wall thicknesses, and dimensions already described, the specific mass ratio, α_T/α_o, can be calculated using equation (C14).

$$\frac{\alpha_T}{\alpha_o} = \frac{t_p}{t_o}\left[\mu_w\left(\frac{t_w}{t_p}\right) + \mu_g\left(\frac{D}{t_p}\right) + \mu_s\left(\frac{t_s}{t_p}\right) + 1\right]$$

$$= \frac{1}{6}\left[\frac{2.163}{4.5} + 3.6\text{x}10^{-5}\left(\frac{1}{0.01}\right) + \frac{1}{2(20)} + 1\right]$$

$$= 0.25$$

Thus the reduction in wall thickness made possible by the window meteoroid bumper results in a 75 percent reduction in the specific mass. It should be remembered that the specific mass includes only the radiating area. It does not include the heat pipe working fluid nor other supporting structure. These parts will be included when M_T/M_0 (eq. (10)) is calculated.

In order to calculate M_T/M_0 the ratios α_T'/α_T and α_0'/α_0 in equation (10) must be known. From the data of reference 14, $\alpha_0'/\alpha_0 = 1.26$. Assuming that the auxiliary material specific masses are the same ($\alpha_T' = \alpha_0$), then $\alpha_T'/\alpha_T = \alpha_0'/\alpha_0(\alpha_0/\alpha_T)$. Using this result plus $\alpha_T/\alpha_0 = 0.25$, $A_T/A_0 = 1.03$, and $\alpha_0'/\alpha_0 = 1.26$ in equation (10) yields $M_T/M_0 = 0.69$. Thus the GPR results in a 31 percent mass reduction from the comparable heat pipe radiator. The masses and areas obtained from these calculations are shown in Table II.

For the hypothetical GPR the wall thicknesses, t_w and t_p were not reduced to the minimum required for meteoroid protection ($t_w + t_p = t_0/6.9$). If t_w, t_p, $t_s \to 0$ then $\alpha_T \to 0$ and the minimum possible mass ratio M_T/M_0 will be obtained. From equation (10) the following is derived,

$$\left.\frac{M_T}{M_0}\right|_{\alpha_T \to 0} = \frac{A_T}{A_0}\,\frac{1}{1 + \dfrac{\alpha_0}{\alpha_0'}}$$

assuming $\alpha_0' = \alpha_T'$. Therefore, for $\alpha_0/\alpha_0 = 1.26$ and $A_T/A_0 = 1.03$,

$$\left.\frac{M_T}{M_0}\right|_{\alpha_T \to 0} = 0.57$$

Thus $M_T/M_0 = 0.69$ obtained for $t_w = t_p = t_s = 0.1$ mm is close to the minimum possible mass ratio $M_T/M_0\,{}_{\alpha_T \to 0} = 0.57$. Therefore, little will be gained by reducing the wall thicknesses further.

V. CONCLUSION

This study was directed at predicting the performance of a new space radiator concept, the gas particle radiator (GPR). The GPR uses a gas containing emitting, submicron particles as the radiating media. The gas particle mixture is contained between the radiator emitting surface and a transparent window. There are two major advantages the GPR has over conventional heat pipe

or pumped loop radiators. First of all, high emissivity is achieved without the use of emissive coatings. Secondly, the GPR potentially has a lower mass.

A radiation heat transfer analysis of the gas particle mixture yielded an expression for the GPR emissivity, ε_T. For a modest volume fraction ($\varphi > 10^{-4}$) of submicron particles and gas thickness ($D \approx 1$ cm) it was found that the emissivity was determined by the window transmittance. Thus the window becomes a critical element in the GPR concept. The window must have high transmittance in the infrared and be strong enough to contain the gas particle mixture. Several candidate window materials are presented in Table I. The listed materials are alkali halides and oxides of silicon, aluminum and magnesium. Another critical issue is maintaining a uniform particle distribution in the gas so that high emissivity is achieved.

Besides determining the emissivity, the window is the critical element for making possible the lower mass for the GPR. The window acts as a "bumper" to provide meteoroid protection for the radiator wall. Thus the combined thickness (window + radiator wall) can be significantly less than the radiator wall thickness alone and still provide the same meteoroid protection. Therefore, the GPR can have a lower mass than a tube type radiator.

The GPR was compared to a proposed titanium wall, potassium heat pipe radiator. For both radiators operating at a power level of 1.01 M_w at 775 K it was found that the GPR mass was 31 percent lower than the heat pipe radiator.

There are many design issues that will have to be addressed and solved to make the GPR a viable space radiator. Two of the most important issues are;

(1) Providing a seal between the window and the emitting radiator surface

(2) A uniform and compatible thermal expansion of the window material and the emitting surface.

Results of this study indicate that the GPR can have a lower mass than tube type radiators without the use of emissive coatings. The window is the critical element for the GPR and must provide high infrared transmittance and sufficient structural strength. Also, to obtain the calculated high emissivity a uniform particle distribution in the gas must be maintained.

APPENDIX A - EMISSIVITY OF GAS-PARTICLE RADIATOR

Approximate the gas particle radiator as an infinite flat plate with gas between the plate and a cover window. Figure (A1) is a schematic of this configuration. In deriving an expression for the spectral emissivity, ε_λ, of the gas-particle radiator the following approximations are used.

(1) Window at uniform temperature, T_w, and behaves in a diffuse manner
(2) Plate at uniform temperature, T_p and behaves in a diffuse manner
(3) Gas at uniform temperature, T_g (no conduction or convection)
(4) Negligible scattering of radiation by particles
(5) Absorption coefficient, k_g, of gas-particle medium is uniform and is determined by particle optical properties (gas is transparent to radiation)
(6) Steady state conditions, $\partial/\partial t = 0$

For the one-dimensional geometry shown in equation (A1) and neglecting conduction and convection the energy equation is the following,

$$\frac{dQ_R}{dx} = 0 \tag{A1}$$

where Q_R is the total radiative heat flux, (W/m^2)

$$Q_R = \int_0^\infty q_\lambda \, d\lambda \tag{A2}$$

And q_λ is the specular heat flux (W/m^2m). As a result of equation (A1)

$$Q_R = \int_0^\infty q_\lambda^p \, d\lambda = \int_0^\infty q_\lambda^w \, d\lambda = \text{constant} \tag{A3}$$

where q_λ^p is the heat supplied to the plate and q_λ^w is the heat leaving the window. The hemispherical spectral emissivity is defined as,

$$\varepsilon_\lambda(T_p,\lambda) = \frac{q_\lambda^w}{\pi B_\lambda^p(T_p,\lambda)} \tag{A4}$$

where B_λ^p is the black body specific intensity,

$$B_\lambda^p(T_p,\lambda) = \frac{2hc^2}{\lambda^5\left(e^{hc/\lambda kT_p} - 1\right)} \tag{A5}$$

Note that ε_λ is defined in terms of the plate temperature, T_p. Also, the total hemispherical emissivity is the following.

$$\varepsilon_T(T_p) = \frac{\pi\int_0^\infty \varepsilon_\lambda B_\lambda^p \, d\lambda}{\sigma T_p^4} = \frac{\int_0^\infty q_\lambda^W \, d\lambda}{\sigma T_p^4} = \frac{Q_R}{\sigma T_p^4} \tag{A6}$$

In order to determine ε_λ and ε_T the heat flux leaving the window, q_λ^W must be found. To obtain q_λ^W the radiative transfer equation must be solved with appropriate boundary conditions. First consider the boundary conditions. Taking a heat balance for a unit area of the window the following is obtained (eq. (A1)).

$$q_{\lambda_i}^W = q_{\lambda_r}^W + q_{\lambda_t}^W + 2\varepsilon_\lambda^W \pi B_\lambda^W \tag{A7}$$

Where $q_{\lambda_i}^W$ is the heat from the gas incident on the window, $q_{\lambda_r}^W$ is the heat reflected from the window back into the gas, $q_{\lambda_t}^W$ the heat transmitted through the window and $2\varepsilon_\lambda^W \pi B_\lambda^W$ is the heat emitted from the window to the gas and to the outside. In obtaining equation (A7) it has been assumed that no heat is being lost by conduction and that no radiation is incident on the window from the outside. The total heat that leaves the window is the following.

$$q_\lambda^W = q_{\lambda_t}^W + \varepsilon_\lambda^W \pi B_\lambda^W \tag{A8}$$

Using equation (A7) to obtain $q_{\lambda_t}^W$ and then substituting in equation (A8) yields the following,

$$q_{\lambda_.}^W = q_{\lambda_i}^W (1 - \rho_\lambda^W) - \varepsilon_\lambda^W \pi B_\lambda^W \tag{A9}$$

where $\rho_\lambda^W \equiv q_{\lambda_r}/q_{\lambda_i}$ is the window reflectivity. Also, since it is assumed that the window behaves in a diffuse manner, the specific radiation intensity leaving the window and entering the gas, $I_{\lambda_o}^W$, can be written in terms of the heat flux $q_{\lambda_o}^W$ as follows.

$$q_{\lambda_o}^W = \int_{\omega=2\pi} I_{\lambda_o}^W \cos\theta \, d\omega = \pi I_{\lambda_o}^W = \rho_\lambda^W q_{\lambda_i}^W + \varepsilon_\lambda^W \pi B_\lambda^W \tag{A10}$$

Now consider an energy balance for a unit area of the emitting plate. (eq. (A1))

$$q_\lambda^p = q_{\lambda_o}^p - q_{\lambda_i}^p \tag{A11}$$

where $q_{\lambda_o}^p$ is the heat leaving the plate and entering the gas and $q_{\lambda_i}^p$ is the heat leaving the gas and striking the plate. Since the plate is assumed to behave in a diffuse manner then a relation similar to equation (A10) for the window is obtained.

$$q_{\lambda_o}^p = \int_{\omega=2\pi} I_{\lambda_o}^p \cos\theta \, d\omega = \pi I_{\lambda_o}^p = \rho_\lambda^p q_{\lambda_i}^p + \varepsilon_\lambda^p \pi B_\lambda^p \tag{A12}$$

The boundary conditions (eqs. (A9) to (A12)) will be applied to the radiative transfer equation (ref. 1). Neglecting scattering, the radiation specific intensity, $I_{\lambda_i}^w(S)$, at the window resulting from radiation within the solid angle, $d\omega$, (fig. (A1)) is the following.

$$I_{\lambda_i}^w(S) = I_{\lambda_o}^p e^{-K_\lambda(S)} + \int_0^{K_\lambda(S)} B_\lambda^g \exp\left[-\left(K_\lambda - K_\lambda^*\right) dK_\lambda^*\right] \tag{A13}$$

Where K_λ is the optical depth,

$$K_\lambda(S) = \int_0^S k_\lambda^g \, ds^* \tag{A14}$$

and k_λ^g is the gas-particle absorption coefficient. Also,

$$S = \frac{D}{\cos\theta} \tag{A15}$$

Therefore, since T_g is assumed uniform (as a result B_λ^g is uniform) and k_λ^g is uniform, equation (A13) becomes the following.

$$I_{\lambda_i}^w = I_{\lambda_o}^p e^{-k_\lambda^g D/\cos\theta} + B_\lambda^g\left[1 - e^{-k_\lambda^g D/\cos\theta}\right] \tag{A16}$$

The heat flux at the window resulting from radiation over all solid angles seen by a point on the window is,

$$q_{\lambda_i}^w = \int_{\omega=2\pi} I_{\lambda_i}^w \cos\theta \, d\omega \tag{A17}$$

Substituting equation (A16) in (A17) yields the following

$$q^{w}_{\lambda_i} = \pi I^{p}_{\lambda_o} \bar{\tau}_\lambda + \pi B^{g}_{\lambda} \bar{\alpha}_\lambda \tag{A18}$$

where $\bar{\tau}_\lambda$ is the gas transmittance and $\bar{\alpha}_\lambda$ is the gas absorptivity.

$$\bar{\tau}_\lambda = \frac{1}{\pi} \int_{\omega=2\pi} e^{-k^{g}_{\lambda} S} \cos\theta \, d\omega = 2 D^2 \int_{S=D}^{\infty} e^{-k^{g}_{\lambda} S} \frac{dS}{S^3} = 2 E_3\left(k^{g}_{\lambda} D\right) \tag{A19}$$

$$\bar{\alpha}_\lambda = \frac{1}{\pi} \int_{\omega=2\pi} \left[1 - e^{-k^{g}_{\lambda} S}\right] \cos\theta \, d\omega = 1 - \bar{\tau}_\lambda = 1 - 2E_3\left(k^{g}_{\lambda} D\right) \tag{A20}$$

and $E_3(x)$ is the exponential integral.

$$E_3(x) = \int_1^{\infty} \frac{1}{u^3} e^{-xu} \, du \tag{A21}$$

Similar to Equation (A18) for the window heat flux, $q^{w}_{\lambda_i}$, the following result is obtained for the plate heat flux,

$$q^{p}_{\lambda_i} = \pi I^{w}_{\lambda_o} \bar{\tau}_\lambda + \pi B^{g}_{\lambda} \bar{\alpha}_\lambda \tag{A22}$$

If the boundary conditions, equations (A10) and (A12) are substituted for $I^{w}_{\lambda_o}$ in equation (A22) and $I^{p}_{\lambda_o}$ in equation (A18) then two equations for $q^{p}_{\lambda_i}$ and $q^{w}_{\lambda_i}$ are obtained. These can be solved to obtain the following result for $q^{w}_{\lambda_i}$.

$$q^{w}_{\lambda_i} = \frac{\pi}{1 - \rho^{p}_{\lambda} \rho^{w-2}_{\lambda} \bar{\tau}_\lambda} \left[B^{g}_{\lambda}\left(1 - \bar{\tau}_\lambda\right)\left(1 + \rho^{p-}_{\lambda} \bar{\tau}_\lambda\right) + B^{p}_{\lambda} \varepsilon^{p-}_{\lambda} \bar{\tau}_\lambda + B^{w}_{\lambda} \varepsilon^{w}_{\lambda} \rho^{p-2}_{\lambda} \bar{\tau}_\lambda\right] \tag{A23}$$

Equation (A23) can now be used in equation (A9) to obtain the heat flux leaving the window, q^{w}_{λ}. Therefore, the spectral emissivity (eq. (A4)) is the following.

$$\varepsilon_\lambda = \frac{q^{w}_{\lambda}}{\pi B^{p}_{\lambda}} = \frac{1 - \rho^{w}_{\lambda}}{1 - \rho^{p}_{\lambda} \rho^{w-2}_{\lambda} \bar{\tau}_\lambda} \left\{\left[1 - \bar{\tau}^{2}_{\lambda}\left(1 - \varepsilon^{p}_{\lambda}\right)\right]\left[\frac{B^{g}_{\lambda}}{B^{p}_{\lambda}} - \frac{\varepsilon^{w}_{\lambda}}{1 - \rho^{w}_{\lambda}} \frac{B^{w}_{\lambda}}{B^{p}_{\lambda}}\right] + \varepsilon^{p-}_{\lambda} \bar{\tau}_\lambda \left[1 - \frac{B^{g}_{\lambda}}{B^{p}_{\lambda}}\right]\right\} \tag{A24}$$

In obtaining equation (A24) Kirchhoff's Law (ref. 1), $\alpha_\lambda = \varepsilon_\lambda$, and the relations

$$\rho_\lambda^p + \alpha_\lambda^p = \rho_\lambda^p + \varepsilon_\lambda^p = 1 \tag{A25}$$

$$\rho_\lambda^w + \alpha_\lambda^w + \tau_\lambda^w = \rho_\lambda^w + \varepsilon_\lambda^w + \tau_\lambda^w = 1 \tag{A26}$$

were used, where ρ_λ is reflectivity, α_λ is absorptivity and τ_λ is transmittance.

The spectral emissivity, ε_λ, was derived under the assumptions given at the beginning of this appendix. Now make the additional assumptions that $T_w = T_g = T_p$ and that the window has negligible emissivity ($\tau_\lambda^w = 1 - \rho_\lambda^w$). Therefore, equation (A24) yields the following.

$$\varepsilon_\lambda = \frac{\tau_\lambda^w}{1 - \rho_\lambda^w \rho_\lambda^{p-2} \tau_\lambda} \left[1 - \tau_\lambda^{-2}\left(1 - \varepsilon_\lambda^p\right)\right] \tag{A27}$$

To obtain the total emissivity, ε_T, equation (A27) is substituted in equation (A6) and the integration is performed. In order to simplify the ε_T calculation the following additional approximations are made; $\varepsilon_\lambda^p << 1$ and $\rho_\lambda^w \rho_\lambda^{p-2} \tau_\lambda << 1$. Using these approximations will result in a value for ε_T lower then the actual value. Therefore, the total emissivity, ε_T, will be a conservative estimate.

$$\varepsilon_\lambda \approx \tau_\lambda^w \left[1 - \tau_\lambda^{-2}\right] \qquad \begin{array}{l}\text{Assumes;} \\ \varepsilon_\lambda^p << 1,\ \rho_\lambda^w \rho_\lambda^{p-2} \tau_\lambda << 1 \\ T_g = T_p,\ \tau_\lambda^w = 1 - \rho_\lambda^w\end{array} \tag{A28}$$

Now consider the total emissivity, ε_T. As discussed in the Emissivity of GPR section, there are two cases to be considered for the absorption coefficient, k_λ^g. For small particles ($r_d/\lambda < 1$) the absorption coefficient is approximated as

$$k_\lambda^g = \frac{K}{\lambda} \varphi \qquad \frac{r_d}{\lambda} < 1 \tag{A29}$$

where K is a constant and φ is the volume fraction of particles in the gas. For large particles ($r_d/\lambda > 1$) it is assumed that the absorption cross section, $\sigma_\lambda^a = \pi r_d^2$, so that,

$$k_\lambda^g = \frac{3}{4}\frac{\varphi}{r_d} \tag{A30}$$

In order to calculate ε_T, an expression for the window transmission, τ_λ^W must be obtained. For these calculations the following result for τ_λ^W will be used.

$$\tau_\lambda^W = \tau_W \quad \text{for} \quad \lambda_\ell \le \lambda \le \lambda_u$$

$$\tau_\lambda^W = 0 \quad \text{for} \quad \lambda < \lambda_\ell \quad \text{and} \quad \lambda > \lambda_u \tag{A31}$$

Also, $\bar{\tau}_\lambda$ (eq. (A19), can be approximated as follows. (Ref. 1).

$$\bar{\tau}_\lambda = 2E_3\left(k_\lambda^g D\right) \approx \exp\left(-1.8k_\lambda^g D\right) \tag{A32}$$

If equations (A28), (A31), and (A32) are now substituted in equation (A6) the following is obtained

$$\varepsilon_T = \frac{\pi\tau_W}{\sigma T_p^4}\int_{\lambda_\ell}^{\lambda_u}\left[1 - \exp\left(-3.6k_\lambda^g D\right)\right] B_\lambda^p \, d\lambda \tag{A33}$$

For the case of large particles (eq. (A30)) k_λ^g is constant and ε_T becomes the following,

$$\varepsilon_T = \tau_W\left[1 - e^{-\beta}\right]\left[F_{o-\lambda_u T_p} - F_{o-\lambda_\ell T_p}\right]; \qquad \frac{r_d}{\lambda} > 1 \tag{A34}$$

$$\beta = 2.7\,\frac{\varphi D}{r_d} \tag{A35}$$

and $F_{o-\lambda T}$ is a tabulated function appearing in many radiation heat transfer texts (ref. 1).

$$F_{o-\lambda T} = \frac{\pi}{\sigma}\int_0^{\lambda T}\frac{B_\lambda(\lambda')}{T^5}\,d(\lambda' T) = \frac{2\pi hc^2}{\sigma}\int_0^{\lambda T}\frac{dx}{x^5\left(e^{hc/kx} - 1\right)} \tag{A36}$$

For window materials to be considered the largest value of $\lambda_\ell \approx 1$ μm, and the highest temperature, T ≈ 1200 K, it is found that $F_{o-1200\ \mu m\ K} < 10^{-2}$. Therefore, the last term in equation (A34) can be neglected and

$$\varepsilon_T = \tau_w F_{o-\lambda_u T_p}(1 - e^{-\beta}) , \qquad \frac{r_d}{\lambda} > 1 \tag{A37}$$

Now consider the case for small particles, $(r_d/\lambda < 1)$. Substituting equation (A29) in (A33) yields the following.

$$\varepsilon_T = \tau_w \left\{ \left[F_{o-\lambda_u T_p} - F_{o-\lambda_\ell T_p} \right] - \frac{2\pi hc^2}{\sigma} \int_{T_p\lambda_\ell}^{T_p\lambda_u} \frac{\exp\left(-\frac{3.6K}{\lambda}\varphi D\right)}{(\lambda T_p)^5 \left[\exp\frac{hc}{k\lambda T_p} - 1\right]} d(\lambda T_p) \right\} \tag{A38}$$

Again the $F_{o-\lambda_\ell T_p}$ term can be neglected. In order to simplify the integration the approximation $\exp(hc/\lambda kT) >> 1$ is made. This will be a good approximation as long as $\lambda_u T_p < 1.4\text{x}10^4$ μm K (ref. 4). With this approximation the integral can be written in terms of the Chi-Square probability function (ref. 15). Therefore,

$$\varepsilon_T = \tau_w \left\{ F_{o-\lambda_u T_p} - \frac{90}{\pi^4}\left(\frac{1}{\gamma + 1}\right)^4 Q\left[\frac{2hc}{\lambda_u k T_p}(\gamma + 1) \middle| 8\right] \right\} , \qquad \frac{r_d}{\lambda} < 1 \tag{A39}$$

where, $Q(x^2|\upsilon)$ is the Chi-Square probability function (ref. 15),

$$Q(x^2|\upsilon) = \left[\Gamma\left(\frac{\upsilon}{2}\right)\right]^{-1} \int_{1/2\ x^2}^{\infty} e^{-t}\ t^{\upsilon/2-1}\ dt \tag{A40}$$

$\Gamma(n)$ is the Gamma function and $\Gamma(n) = (n - 1)!$ for n an integer. The parameter γ appearing in equation (A39) is the following.

$$\gamma = \frac{3.6KkT_p}{hc}\varphi D \tag{A41}$$

In equation (A39) the term $Q[2hc/\lambda_\ell kT_p(\gamma + 1)|8]$ has been neglected since for $\lambda_\ell \approx 1$ μm and $T_p \approx 1200$ K, this term is less than 10^{-2}.

APPENDIX B - TEMPERATURE DIFFERENCE BETWEEN PARTICLES AND SURROUNDING GAS

Consider a particle to be approximated by a sphere of radius, r_d. The surface of the sphere is at temperature, T_{rad}, and is surrounded by a gas at temperature, T_g, and moving with velocity, V.

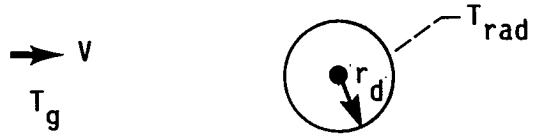

For steady state conditions the heat transfer to the sphere will equal the heat radiated by the sphere. Therefore,

$$hA_s(T_g - T_{rad}) = \sigma\varepsilon_s A_s\left(T_{rad}^4 - T_\infty^4\right) \tag{B1}$$

where h is the heat transfer coefficient, A_s, is the surface area of the sphere, $\sigma(= 5.7\text{x}10^{-8}$ watts/m^2 $K^4)$ is the Stefan-Boltzmann constant, ε_s is the sphere emissivity, and T_∞ is the radiation sink temperature. Absorption by the surrounding gas, which will lessen the temperature difference, $T_g - T_{rad}$, is being neglected in equation (B1). Since the largest temperature difference is of interest here, neglecting gas absorption is a conservative approximation. From Eq. (B1) the temperature difference is

$$\Delta T \equiv (T_g - T_{rad}) = \Theta\left(T_{rad}^4 - T_\infty^4\right) \tag{B2}$$

The parameter,

$$\Theta = \frac{\sigma\varepsilon_s}{h} \tag{B3}$$

will determine ΔT.

The heat transfer coefficient, h, depends upon the flow conditions. For the case of very small particles the mean free path of the gas molecules, ℓ_g, will be the same order of magnitude as r_d. In this case the heat transfer to the particle will be described by free molecular flow. In the case of large particles, $\ell_g \ll r_d$, and the heat transfer will be determined by continuum flow. First consider the free molecular flow case, $(\ell_g/r_d \geq 1)$. The energy transfer to the sphere is the following.

$$Q = \int_s (E_i - E_r)\, dS \tag{B4}$$

Where E_i is the energy of the gas molecules striking the sphere and E_r is the energy flux of the gas molecules reflected from the sphere. From the definition of the thermal accommodation coefficient (ref. 16), α,

$$\alpha \equiv \frac{E_i - E_r}{E_i - E_w} \tag{B5}$$

where E_w is the energy flux of gas molecules that have completely accommodated to the sphere wall temperature, T_{rad}. Using equation (B5) in (B4) yields the following.

$$Q = \alpha \int_S (E_i - E_w)\, dS \tag{B6}$$

Now consider expressions for E_i and E_w. The energy fluxes, E_i and E_w consist of two parts; the kinetic energy flux, E', and the internal energy, E", carried by the gas molecules. The kinetic energy flux, E', is given by

$$E' = \int_0^\infty dc_x \int_{-\infty}^\infty dc_y \int_{-\infty}^\infty \frac{1}{2} m_g c^2 c_x F\, dc_z \tag{B7}$$

where $c^2 = c_x^2 + c_y^2 + c_z^2$ is the gas molecule velocity squared and F is the distribution function. Assume a Maxwellian distribution function and since the flow velocity, V, is small compared to the thermal speed, c_m,

$$c_m^2 = \frac{2kT}{m_g} \tag{B8}$$

the following results for F.

$$F = \frac{n_g}{\sqrt{\pi c_m^3}} \exp\left(-\frac{c_x^2 + c_y^2 + c_z^2}{c_m^2}\right) \tag{B9}$$

Using equation (B9) in (B7) yields the following.

$$E' = \dot{n}(2kT) \tag{B10}$$

Where $\dot{n}$ is the gas molecular flux,

$$\dot{n} = \frac{1}{4} n \sqrt{\frac{8kT}{\pi m_g}} \tag{B11}$$

and n is the gas number density. The internal energy flux, E", is the following,

$$E'' = j\left(\frac{kT}{2}\right)\dot{n} \tag{B12}$$

where j is the number of degrees of freedom of the gas molecules which can be written in terms of the specific heat ratio, γ, as follows.

$$j = \frac{5 - 3\gamma}{\gamma - 1} \tag{B13}$$

Using equations (B10), (B11), and (B12) yields the following (ref. 16).

$$E_i = E_i' + E_i'' = \frac{\gamma + 1}{2(\gamma - 1)}\,\dot{n}_i kT_g \tag{B14}$$

$$E_w = E_w' + E_w'' = \frac{\gamma + 1}{2(\gamma - 1)}\,\dot{n}_r kT_{rad} \tag{B15}$$

Since the flux of incident molecules, $\dot{n}_i$, must equal the flux of reflected molecules, $\dot{n}_r$, the following result is obtained.

$$E_i - E_w = \frac{\gamma + 1}{2(\gamma - 1)}\,\dot{n}_i k(T_g - T_{rad}) \tag{B16}$$

$$\dot{n}_i = \frac{1}{4}\,n_g\sqrt{\frac{8kT_g}{\pi m_g}} \tag{B17}$$

Assuming T_{rad} is uniform on the particle surface, the following is obtained for Q by substituting equation (B16) in (B6).

$$Q = \frac{\alpha(\gamma + 1)}{8(\gamma - 1)}\,n_g\sqrt{\frac{8kT_g}{\pi m_g}}\,k(T_g - T_{rad})A_s \tag{B18}$$

From this the heat transfer coefficient is the following.

$$h_f = \frac{\alpha(\gamma + 1)}{8(\gamma - 1)}\,n_g k\sqrt{\frac{8kT_g}{\pi m_g}} \tag{B19}$$

Now consider the continuum flow heat transfer case. For low speed flow (Oseen Flow) the Nusselt number for a sphere is the following (ref. 17),

$$Nu_c \equiv \frac{2r_d}{\lambda_{th}}\,h_c \approx 2 \tag{B20}$$

for small Reynolds number. Appearing in equation (B20) are the continuum heat transfer coefficient, h_c, and the gas thermal conductivity, λ_{th}. From equation (B20) the following is obtained.

$$h_c = \frac{\lambda_{th}}{r_d} \tag{B21}$$

The thermal conductivity is the following (ref. 18),

$$\lambda_{th} = \frac{75}{8} k \sqrt{\frac{kT_g}{m_g}} \frac{1}{\Sigma_g} \tag{B22}$$

where Σ_g is the velocity averaged cross section ($\Sigma_g = 8\pi d_g^2$ for hard spheres, where d_g is the gas molecule diameter). If equation (B22) is used in (B21) and the result combined with equation (B19), the following is obtained.

$$\frac{h_c}{h_f} = \frac{75(\gamma - 1)}{\alpha(\gamma + 1)} \sqrt{\frac{\pi}{8}} \left(\frac{\ell_g}{r_d}\right) \tag{B23}$$

Where ℓ_g is the gas mean free path.

$$\ell_g = \frac{1}{n_g \Sigma_g} \tag{B24}$$

Now consider an estimate of the parameter, θ, for the gas particle radiator. For helium at $T_g = 1000$ K, and a pressure, $p_g = 0.1$ atm, ($n_g = p_g/kT_g$) and $\gamma = 5/3$, equation (B19) gives the following result.

$$h_f = 1.2\text{x}10^4 \, \alpha \qquad \text{watts/m}^2 \text{ K} \tag{B25}$$

Also, using equation (23) the following is obtained.

$$h_c = 1.4\text{x}10^5 (\ell_g/r_d) \qquad \text{watts/m}^2 \text{ K} \tag{B26}$$

Therefore,

$$\theta_f = \frac{\sigma \varepsilon_s}{h_f} = 4.8\text{x}10^{-12} \frac{\varepsilon_s}{\alpha} \qquad 1/\text{K} \tag{B27a}$$

$$\theta_c = \frac{\sigma \varepsilon_s}{h_c} = 4.2\text{x}10^{-13} \left(r_d/\ell_g\right) \varepsilon_s \qquad 1/\text{K} \tag{B27b}$$

Assume $\varepsilon_s/\alpha \approx 1$, also for $p_g = 0.1$ atm and $\Sigma_g \approx 10^{-15}$ cm^2, $\ell_g \approx 10$ μm so that for $r_d \approx 100$ μm, $r_d/\ell_g \approx 10$. Therefore, $\theta_f \approx 4.8\times10^{-12}$, and assuming $\varepsilon_s \approx 1$, $\theta_c \approx 4.1\times10^{-12}$. Neglecting T_∞^4 in equation (B2) yields the following.

$$\frac{\Delta T}{T_{rad}} = \theta T_{rad}^3 \tag{B28}$$

Using the above values for θ_f and θ_c the following is obtained for $T_{rad} = 1000$ K

$$\left.\frac{\Delta T}{T_{rad}}\right|_f < 0.01 \qquad \left.\frac{\Delta T}{T_{rad}}\right|_c < 0.01 \tag{B29}$$

Therefore, for both free molecular flow and continuum flow the temperature difference will be less than 1 percent and can be neglected.

APPENDIX C - SPECIFIC MASS COMPARISON OF GAS PARTICLE AND TUBE RADIATORS

Consider one segment of the gas particle radiator to consist of a metal tube surrounded by a transparent window as shown in equation (C1). The window is attached to the tube by vertical members that are spaced a distance L apart. Therefore, the total mass of the radiator section, m_t, not including the mass of the radiator working fluid (wick and fluid mass for a heat pipe) is the following

$$m_T = \rho_w V_w + \rho_p V_p + V_g\left(\rho_g + \varphi\rho_d\right) + \rho_s V_s \tag{C1}$$

Where ρ_w is the density of the window material, V_w is the volume of window material, ρ_p is the density of the tube material, V_p is the volume of tube material, V_g is the gas volume, ρ_g is the gas density, φ is the volume fraction of particles, ρ_d is the particle density, V_s is the volume of the attachment member, and ρ_s is the density of the attachment member. Referring to figure (C1), the volumes are the following.

$$V_w = \pi L t_w (2R_w + t_w) \tag{C2}$$

$$V_p = \pi L t_p (2R_p + t_p) \tag{C3}$$

$$V_g = \pi L\left(R_w^2 - R_p^2 - 2t_p R_p - t_p^2\right) \tag{C4}$$

$$V_s = \pi t_s\left(R_w^2 - R_p^2\right) \tag{C5}$$

Where t denotes material thickness, R denotes radius, and L is the length of the radiator segment.

Now define the specific mass, α_T, in terms of the tube surface area.

$$\alpha_T \equiv \frac{m_T}{2\pi R_p L} \tag{C6}$$

Substitute equations (C1) to (C5) in (C6). Therefore, making the approximation $t_w \ll R_w$ and $t_p \ll R_p$ the following result is obtained,

$$\alpha_T = \rho_w t_w\left(\frac{R_w}{R_p}\right) + \rho_p t_p + \frac{1}{2}\left(\rho_g + \varphi\rho_d\right)\left(1 + \frac{R_w}{R_p}\right)D + \frac{1}{2}\rho_s t_s\left(1 + \frac{R_w}{R_p}\right)\frac{D}{L} \tag{C7}$$

where

$$D \equiv R_w - R_p \tag{C8}$$

For a simple tube radiator of thickness, t_o, and density, ρ_o, the specific mass, α_o, will include only the second term in equation (C7).

$$\alpha_o \equiv \frac{m_o}{2\pi R_o L} = \rho_o t_o \tag{C9}$$

Now divide equation (C7) by (C9) so that the following result is obtained.

$$\frac{\alpha_T}{\alpha_o} = \mu_w\left(\frac{t_w}{t_o}\right) + \mu_g\left(\frac{D}{t_o}\right) + \mu_s\left(\frac{t_s}{t_o}\right) + \frac{\rho_p}{\rho_o}\left(\frac{t_p}{t_o}\right) \tag{C10}$$

where,

$$\mu_w \equiv \frac{\rho_w}{\rho_o}\frac{R_w}{R_p} \tag{C11}$$

$$\mu_g \equiv \frac{\rho_g + \rho_d\varphi}{2\rho_o}\left(1 + \frac{R_w}{R_p}\right) \tag{C12}$$

$$\mu_s \equiv \frac{1}{2}\frac{\rho_s}{\rho_o}\left(\frac{D}{L}\right)\left(1 + \frac{R_w}{R_p}\right) \tag{C13}$$

for the case where the same tube material is used for both the gas particle and simple tube radiator ($\rho_o = \rho_p = \rho_s$) then equation (C10) becomes the following.

$$\frac{\alpha_T}{\alpha_o} = \mu_w\left(\frac{t_w}{t_o}\right) + \mu_g\left(\frac{D}{t_o}\right) + \mu_s\left(\frac{t_s}{t_o}\right) + \left(\frac{t_p}{t_o}\right) \tag{C14}$$

Where, since $\rho_s = \rho_o$

$$\mu_s = \frac{1}{2}\left(\frac{D}{L}\right)\left(1 + \frac{R_w}{R_p}\right) \tag{C15}$$

If a flat plate radiator is being considered rather then a cylindrical geometry then,

$$\mu_w \equiv \frac{\rho_w}{\rho_o} \tag{C16}$$

$$\mu_g \equiv \frac{\rho_g}{\rho_o} + \varphi\left(\frac{\rho_d}{\rho_o}\right) \tag{C17}$$

$$\mu_s \equiv \frac{1}{2}\left(\frac{D}{L}\right) \tag{C18}$$

D = distance between emitting plate and window (C19)

REFERENCES

1. Siegel, R.; and Howell, J.R.: Thermal Radiation Heat Transfer. 2nd ed., McGraw Hill, New York, 1981.
2. Lundeberg, J.F.; Stern, P.H.; and Bristow, R.J.: Meteoroid Protection for Spacecraft Structures. Boeing Co, Seattle, WA, D2-25056, Oct. 1965. (NASA CR-54201).
3. Humes, D.H.: Meteriod Bumper Experiment on Explorer 46. NASA TP-1879, 1981.
4. Lanzo, C.D.; and Ragsdale, R.G.: Experimental Determination of Spectral and Total Transmissivities of Clouds of Small Particles. NASA TN D-1405, 1962.
5. Howell, J.R.; and Renkel, H.E.: Analysis of the Effect of a Seeded Propellant Layer on Thermal Radiation in the Nozzle of a Gaseous-Core Nuclear Propulsion System. NASA TN D-3119, 1965.
6. Siegel, R.: Radiative Behavior of a Gas Layer Seeded with Soot. NASA TN D-8278, 1976.
7. Touloukian, Y.S.; and DeWitt, D.P.: Thermophysical Properties of Matter. Vol. 8, Thermal Radiative Properties, Nonmetallic Solids, Plenum Press, New York, 1972.
8. Weast, R.C., ed.: Handbook of Physics and Chemistry. 64th ed., CRC Press, Boca Raton, FL, 1983.
9. Drexhage, M.G.; and El-Bayoumi, O.H.: Heavy-Metal Flouride Glasses for Mid-IR Military Applications," Aerospace America, Vol. 23, No. 4, Apr. 1985, pp. 66-69.
10. Mimura, Y.; Ohamura, Y.; and Ota, C.: Single-Crystal CsBr Infrared Fibers. Journal of Applied Physics, Vol. 53, No. 8, Aug. 1982, pp. 5491-5497.
11. Chin, G.Y.; Van Uitert, L.G.; Green, M.L.; and Zydzik, G.: Hardness, Yield Strength and Young's Modulus in Halide Crystals. Scripta Metallurgica, Vol. 6, No. 6, 1972, pp. 475-480.

12. Ahlquist, C.N.: The Influence of Yield Strength on Fracture of Semi-Brittle Ceramic Crystals. Acta Metallurgica, Vol. 22, No. 9, Sept. 1974, pp. 1133-1137.
13. Meteoroid Damage Assessment. NASA SP-8042, 1970.
14. Girrens, S.P.: Design and Development of a Titanium Heat-Pipe Space Radiator. Los Alamos Report LA-9251-MS, Mar, 1982.
15. Abramowitz, M.; and Stegun, I.A., eds.: Handbook of Mathematical Functions with Formulas, Graphs, and Mathematical Tables. National Bureau of Standards Applied Mathematics Series, No. 55, 1964.
16. Schaaf, S.A.; and Chambre, P.L.: Flow of Rarefied Gases. Fundamentals of Gas Dynamics, ed. by E.W. Emmons, Vol. III of High Speed Aerodynamics and Jet Propulsion, Princeton University Press, Princeton, NJ, 1958, pp. 687-739.
17. White, F.M.: Viscous Fluid Flow. McGraw Hill, New York, 1974, p. 213.
18. Burgers, J.M.: Flow Equations for Composite Gases. Academic Press, New York, 1969, p. 68.

TABLE I. - CANDIDATE WINDOW MATERIALS

Material	Transmission range		Transmittance	Density, gm/cm^3	Melting point, °C	Water solubility, gm/100 gm	(Type) Yield stress, N/mm^2 (lb/in^2)
	λ_ℓ, μm	λ_u, μm	Material thickness, mm				
Fused silica (SiO_2)	0.25	3.5	>0.9 (5)	2.65	1610	Insol.	----------
Sodium chloride (NaCl)	.35	15	>.9 (5)	2.165	801	35.7	(Compressive)[11] 0.69 to 41.3 (100 to 6000)
Silver chloride (AgCl)	.4	20	.8 (.5)	5.56	455	0.0021	----------
Calcium fluoride (CaF_2)	.25	8	.95 (1-11)	3.18	1423	.0017	----------
Lithium fluoride (LiF)	.2	5.5	.95 (1-3)	2.635	845	.27	(Shear)[12] 1.2 to 6.0 (174 to 870)
Sodium fluoride (NaF)	.3	10	>.9 (2.16)	2.558	993	4.22	----------
Potassium bromide (KBr)	.5	20	>.9 (4)	2.75	734	102	(Compressive)[11] 0.69 to 40 (10 to 5800)
Cesium bromide (CsBr)	1	25	.9 (10)	3.04	636	123	(Compressive)[10] 22.5 (3270)
Aluminum oxide (Al_2O_3, crystal)	.3	4	.85 (0.5)	4.0	2316	Insol.	----------
Magnesium oxide (MgO, crystal)	.6	6	.85 (1-9)	3.77	3223	Insol.	(Shear)[12] 36 (5225)
Cesium iodide (CsI, crystal)	1	40	.9 (5-10)	4.51	626	160	----------
Heavy-metal fluoride glasses (HMFG)							
$HF_4 \cdot BaF_2 \cdot LaF_3 \cdot AlF_3$	.3	7	.9	5.88	312	------	----------
$BaFe \cdot ZnF_2 \cdot LaF_3 \cdot TnF_4$	.3	9	.9	6.2	357	------	----------

TABLE II. - COMPARISON BETWEEN HEAT PIPE RADIATOR AND GAS PARTICLE RADIATOR

[Radiator conditions; radiated power = 1.01 MW, radiator temperature = 775 K].

	Radiator area, A, m^2	Radiating surface mass, $M_{rad} = \alpha A$, kg	Auxiliary mass, $M_a = \alpha' A$, kg	Total mass, $M_{rad} + M_a$, kg
Heat pipe radiator (ref. 14)	67	170	214	384
Gas particle radiator	69	44	221	265

Titanium wall potassium heat pipe data (ref. 14): Emissivity, $\epsilon_0 = 0.9$; radiating wall thickness, $t_0 = 0.6$ mm; area redundancy, $r = 321/360$

Gas particle radiator data: Emissivity, $\epsilon_T = 0.84$, NaCl window ($\lambda_u = 15$ μm, $\tau_w = 0.9$); wall thicknesses, $t_p = t_w = t_s = 0.1$ mm; area redundancy, $r = 321/360$; redundant area emissivity, $\epsilon_T' = 0.3$; helium pressure, $p_g = 15$ torr.

Calculated results used to obtain GPR results:

$$\frac{\alpha_T}{\alpha_0} = 0.25 , \qquad \frac{A_T}{A_0} = 1.03 , \qquad \frac{\alpha_0'}{\alpha_0} = \frac{\alpha_T'}{\alpha_0} = 1.26$$

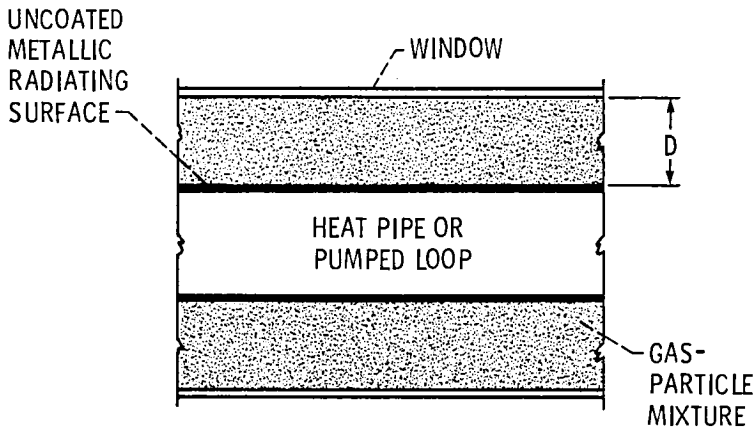

Figure 1. - Gas particle radiator concept.

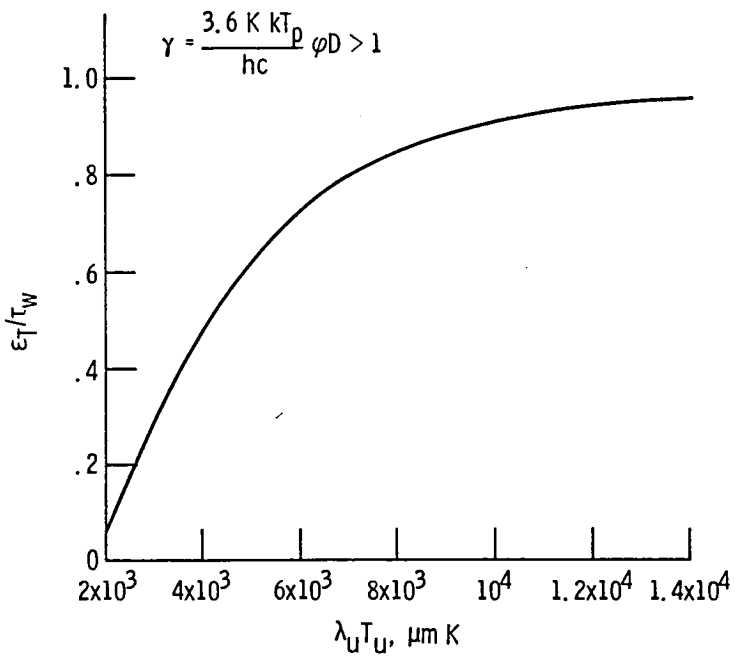

Figure 2. - Total emissivity for small particles ($r_d < 1$ μm, $T_p \leq 1200$ K).

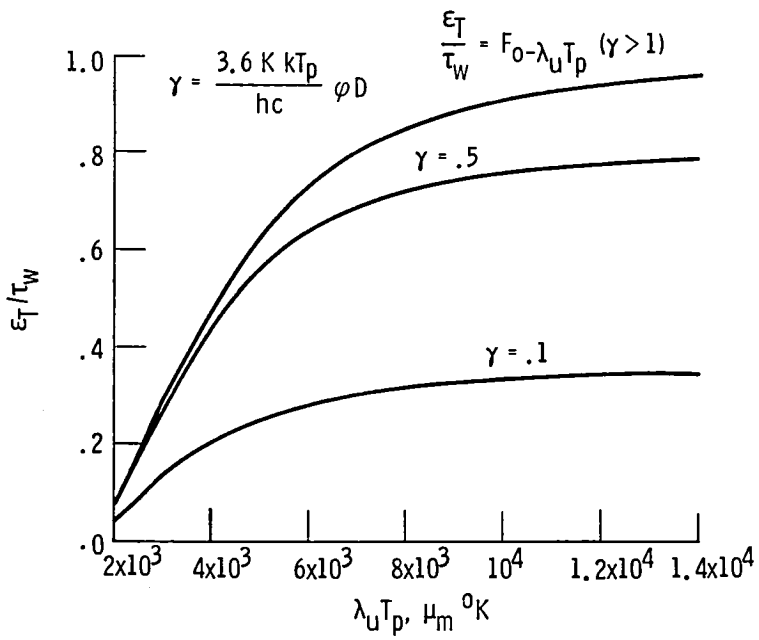

Figure 3. - Total emissivity for small particles ($r_d < 1$ μm, $T_p \leq 1200$ K).

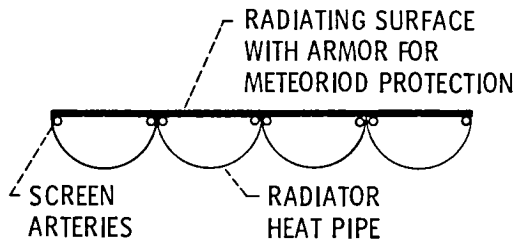

(a) Cross section of heat pipe radiator of Ref. 14.

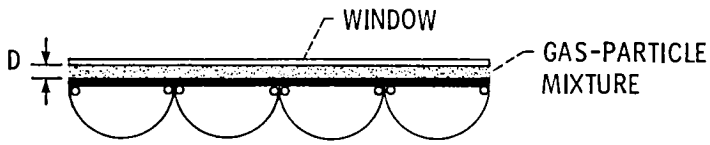

(b) Heat pipe radiator modified to produce a gas-particle radiator.

Figure 4. - Cross-section of heat pipe radiator of Ref. 14 and modification to produce a gas-particle radiator.

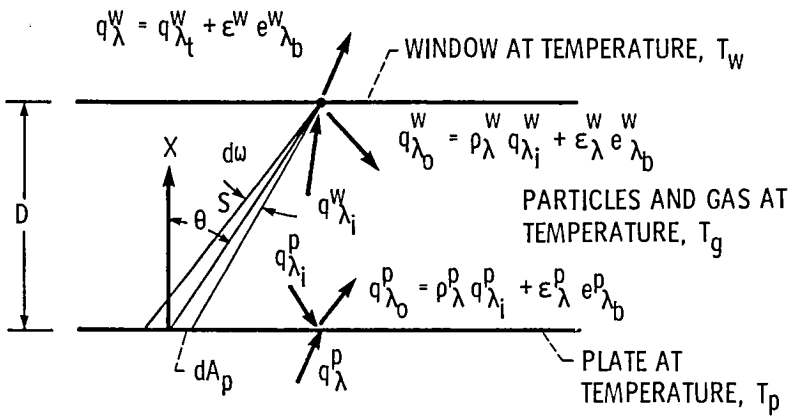

Figure A1. - Schematic of gas-particle radiator.

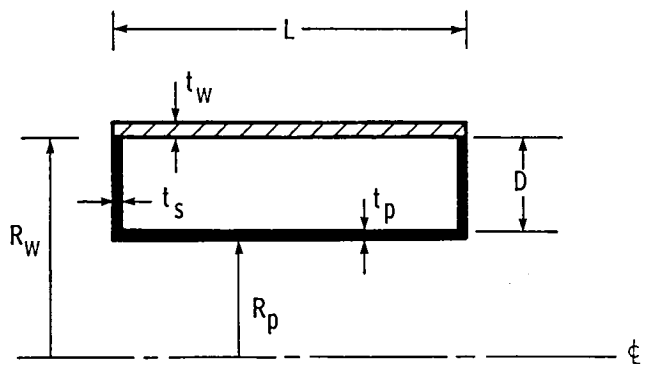

Figure C1. - Schematic of cylindrical gas particle radiator.

1. Report No.	2. Government Accession No.	3. Recipient's Catalog No.
NASA TM-88786		

4. Title and Subtitle	5. Report Date
Analysis of the Gas Particle Radiator	July 1986
	6. Performing Organization Code: 506-41-11
7. Author(s): Donald L. Chubb	8. Performing Organization Report No.: E-2639-1
	10. Work Unit No.
9. Performing Organization Name and Address: National Aeronautics and Space Administration, Lewis Research Center, Cleveland, Ohio 44135	11. Contract or Grant No.
12. Sponsoring Agency Name and Address: National Aeronautics and Space Administration, Washington, D.C. 20546	13. Type of Report and Period Covered: Technical Memorandum
	14. Sponsoring Agency Code

15. Supplementary Notes

16. Abstract

Theoretical performance of a new space radiator concept, the gas particle radiator (GPR), is calculated. The GPR uses a gas containing emitting, submicron particles as the radiating media. A transparent window contains the gas particle mixture around the solid radiator emitting surface. A major advantage of the GPR is that large emissivity ($\epsilon_T \geq 0.8$) is achieved without the use of emissive coatings. A radiation heat transfer analysis shows that for a modest volume fraction ($\sim 10^{-4}$) of submicron particles and gas thickness ($\sim$1 cm) the emissivity, ϵ_T, is limited by the window transmittance. Besides determining the emissivity, the window is the critical element for making it possible for the GPR to have lower mass than a tube type radiator. The window acts as a "bumper" to provide meteoroid protection for the radiator wall. The GPR was compared to a proposed titanium wall, potassium heat pipe radiator. For both radiators operating at a power level of 1.01 MW at 775 K it was calculated that the GPR mass was 31 percent lower than the heat pipe radiator.

17. Key Words (Suggested by Author(s))	18. Distribution Statement
Space radiator	Unclassified - unlimited STAR Category 20

19. Security Classif. (of this report)	20. Security Classif. (of this page)	21. No. of pages	22. Price*
Unclassified	Unclassified		

*For sale by the National Technical Information Service, Springfield, Virginia 22161

National Aeronautics and
Space Administration

Lewis Research Center
Cleveland, Ohio 44135

SECOND CLASS MAIL

ADDRESS CORRECTION REQUESTED

Official Business
Penalty for Private Use $300

Postage and Fees Paid
National Aeronautics and
Space Administration
NASA-451

NASA